Single-Electron Capacitance Spectroscopy of Discrete Quantum Levels

R. C. Ashoori, H. L. Stormer, J. S. Weiner, L. N. Pfeiffer, S. J. Pearton, K. W. Baldwin, and K. W. West
AT&T Bell Laboratories, Murray Hill, New Jersey 07974
(Received 2 March 1992)

We observe the capacitance signal resulting from single electrons tunneling into discrete quantum levels. The electrons tunnel between a metallic layer and confined states of a single disk in a microscopic capacitor fabricated in GaAs. Charge transfer occurs only for bias voltages at which a quantum level resonates with the Fermi energy of the metallic layer. This creates a sequence of distinct capacitance peaks whose bias positions directly reflect the electronic spectrum of the confined structure. From the magnetic field evolution of the spectrum, we deduce the nature of the bound states.

PACS numbers: 73.20.Dx, 71.50.+t, 71.55.−i, 72.20.My

Man-made microstructures which confine electrons arbitrarily in all three spatial dimensions provide uniquely simple model systems for the study of few particle physics. Direct spectroscopy of the quantum states of individual microstructures has been sought as a probe of their electronic properties. McEuen *et al.* [1] have demonstrated a transport spectroscopy on a small system containing ~100 electrons which is sensitive to charging effects [2] (Coulomb blockade) as well as to quantum level splittings. Others have studied quantum dots fabricated from double barrier resonant tunneling structures and report the observation of quantum level splittings [3] and single-electron charging effects [4]. However, this latter technique is difficult to exploit as a spectroscopic tool since the devices operate far from equilibrium. Far-infrared [5] and conventional capacitance [6,7] spectroscopies have been performed but require large arrays of nominally identical nanostructures in order to provide measurable signals. As it turns out, the interpretation of such data suffers from unavoidable structure to structure inhomogeneity [8].

This Letter describes capacitance spectroscopy on a GaAs tunnel capacitor [9] containing only a *single* microscopic region for charge accumulation. The charge in this region can be varied from zero to several thousand electrons. We observe discrete peaks in the device capacitance as a function of voltage across the capacitor. The peaks are caused by single electrons tunneling between a metallic layer and discrete quantum levels laterally confined in a quantum well. The gate bias positions of these peaks are determined by the energetics of electron charging and the quantum level structure in the tunnel capacitor [8]. Moreover, the gate bias scale can be directly converted to an energy scale in the quantum well.

The tunnel capacitor is fabricated from a GaAs/AlGaAs multilayer wafer grown by molecular beam epitaxy. The layer sequence is as follows: 1-μm undoped GaAs buffer layer; 3000-Å n^+ (4×10^{17} cm^{-3}) GaAs; 150-Å undoped GaAs spacer layer; 85-Å $Al_{0.3}Ga_{0.7}As$ tunnel barrier; 150-Å GaAs quantum well; 150-Å $Al_{0.3}Ga_{0.7}As$ undoped setback; 350-Å n doped $Al_{0.3}Ga_{0.7}As$ region; 300-Å undoped GaAs cap layer. The conduction band profile in these layers is pictured in Fig. 1(a), and a cross section through a processed device is shown in Fig. 1(b). A 1-μm-diam CrAu disk is fabricated using electron beam lithography. After a 300-Å dry etch, a 2-μm-diam CrAu disk, shown in Fig. 1(c), is patterned to cover the 1-μm disk. A narrow lead connects the 2-μm disk (gate) to nearby electronics. Depletion under the etched surface confines electrons to the region of the well under the 1-μm disk [10].

To measure the capacitance signal from single electrons moving back and forth across the tunnel barrier, we have incorporated our device into a "bridge on a chip," with a standard capacitor and detector located very close to the tunnel capacitor. The circuit is shown schematically in Fig. 1(d). ac excitation voltages differing in phase by 180° are applied to the n^+ layer of the tunnel capacitor, C_T, and to one plate of the on-chip standard capacitor, C_S. The gate of C_T and the other plate of C_S are electrically connected, and the signal is measured at this "balance point" of the bridge. As a detector, we use a

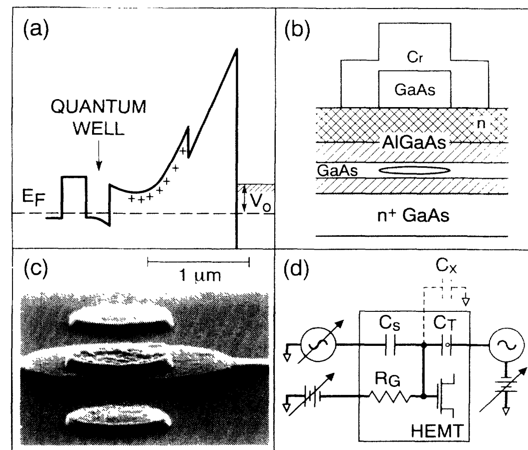

FIG. 1. (a) Conduction band profile of the multilayer sample. E_F is the Fermi level in the n^+ doped bottom layer. V_0 is the voltage applied to the gate. (b) Schematic cross section through the tunnel capacitor. (c) SEM photograph of the tunnel capacitor showing the top gate. (d) Low-temperature, on-chip capacitance bridge (box) and external circuit.

cryogenic high electron mobility transistor (HEMT) with input shunt capacitance C_G of ≈ 0.3 pF. It is positioned within 2 mm of the bridge and mounted in a fashion which leaves its characteristics practically unaffected by an applied magnetic field. The bias on the gate of the transistor is established through a nearby 20-MΩ thin-film resistor, R_G.

The transistor can be thought of as an impedance matcher operating around unity voltage gain. With a low capacitance input, it drives high capacitance lines. To obtain high sensitivity, care was taken to minimize the shunting capacitance C_{shunt} (the sum of C_S, C_T, C_G, and stray capacitance C_X), from the balance point. The signal from the HEMT is further amplified and fed into a lock-in amplifier. Initially, the on-chip bridge is balanced by adjusting the ac voltage amplitude on the standard capacitor. The experiment consists of monitoring the off-null signal at the balance point as the dc bias across the tunnel capacitor is varied. All data are taken with a 210-kHz excitation at pumped ^{3}He temperatures.

With a 20-MΩ gate bias resistor, the RC time constant at the balance point is ≈ 20 μs. This is much longer than the $1/\omega = 0.8$ μs of the ac excitation. Therefore our bridge is sensitive to charge induced on the gate of the tunnel capacitor resulting from electron tunneling between the n^+ layer and the quantum well in synchrony with the ac excitation. The noise level for detection of charge on the balance point is $\approx 3\times10^{-2}e/\sqrt{\text{Hz}}$, rivaling that of early double junction single-electron devices [2].

The inset of Fig. 2 shows the capacitance of the tunnel capacitor as a function of gate bias after subtraction of a linear background of ≈ 1 fF/V. This background results from a small depletion of the metallic n^+ layer under negative gate bias. A sharp rise in the capacitance is apparent around -450 mV. The same feature is observed in measurements on a large area device fabricated from the same wafer. This capacitance step develops as electrons from the n^+ layer fill up the quantum well, reducing the effective distance between the capacitor plates. At high (positive direction) gate biases, the device contains a disk of electrons of 1 μm diam in the quantum well, whereas at low gate biases this area is totally depleted. The calculated capacitance step height from this filling is ≈ 0.25 fF, which calibrates the vertical scale of the inset and yields $C_{\text{shunt}} = 0.9 \pm 0.1$ pF.

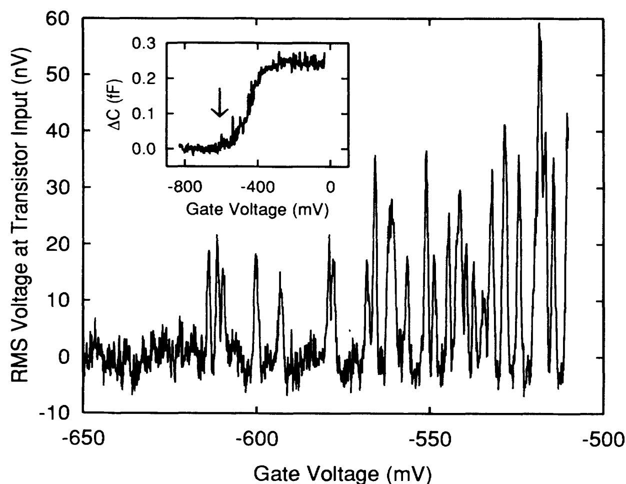

FIG. 2. The rms signal at the input of the HEMT as a function of gate bias using a 0.33-mV excitation. A linear background has been subtracted. Inset: Device capacitance measured at 0.9-mV rms excitation. The arrow indicates the position of the first peak of the main figure.

Figure 2 shows the device capacitance as measured with high resolution at gate biases below the capacitance step. We observe a sequence of well-resolved and reproducible capacitance peaks whose positions only change upon thermal cycling. In the example of Fig. 2, the first peak appears at -614 mV, and there exist no such features at lower voltages. The small peaks of Fig. 2 are of similar height (15–20 nV rms) and width (≈ 1 mV) with taller peaks of variable width and height increasingly appearing at higher gate bias. The small capacitance peaks arise from single electrons tunneling into the lowest energy discrete quantum states of the gated region in the quantum well. The taller peaks are caused by near or actual degeneracies in gate bias at which several electrons tunnel into the disk. The positions of these peaks reflect directly the energetics of the quantum levels.

In our tunnel capacitor, near an isolated capacitance peak, at most one electron is induced to tunnel between the n^+ layer and the discrete state in the well. The electron travels only a fraction, $1/\eta$, of the distance between the plates of the tunnel capacitor. Therefore the amount of charge induced on the gate due to a single electron tunneling is $-e/\eta$, which translates to a voltage change at the balance point of $-e/\eta C_{\text{shunt}}$. We refer to η as the "lever arm." Its value is given by $\eta \approx 4.0$ as determined from the molecular beam epitaxy (MBE) growth parameters and capacitance measurements on large area mesas. The lever arm also sets the reduction factor between externally applied voltage V_0 and the voltage drop between the n^+ layer and the quantum well. This establishes the energy scale $E = eV_0/\eta$ for the well as is evident from Fig. 1(a).

For an electron, the mean time for tunneling between the n^+ layer and the well is less than 0.1 μs. During one cycle of the excitation an electron can tunnel many times back and forth through the barrier. Although each tunneling process transfers a complete electron charge, the occupation of the quantum level appears to be continuous and reflects the Fermi distribution in the n^+ electrode.

In order to convince ourselves of the validity of this picture, we analyze in detail the behavior of an individual peak as the excitation amplitude is varied. The top curve of the left inset of Fig. 3 shows the voltage change at the balance point due to tunneling as the bias voltage is scanned through a capacitance peak. It is just the Fermi

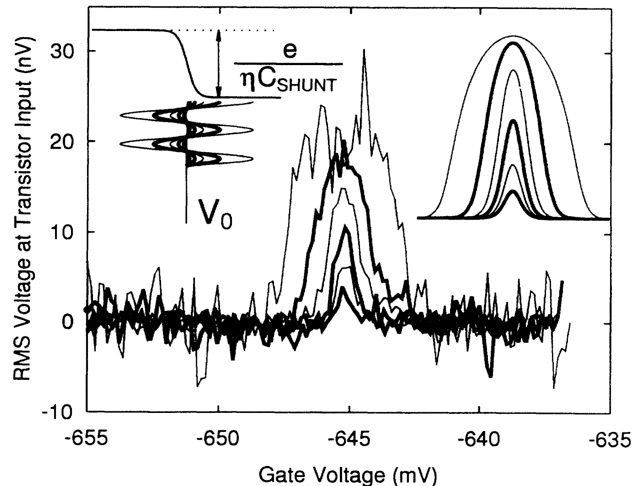

FIG. 3. The rms signal at the HEMT input for a sequence of sinusoidal excitation voltages. The smallest excitation is 0.056 mV rms. In each subsequent curve the excitation amplitude V_{ac} increases by a factor of 2. Left inset: Representation of the voltage response at the HEMT to ac excitations of varying amplitude. For details see text. The sinusoids depict the different ac excitation amplitudes used in the experiment. Right inset: Results of the model calculation for the different excitation amplitudes used in the main figure, assuming $C_{\text{shunt}}=0.9$ pF.

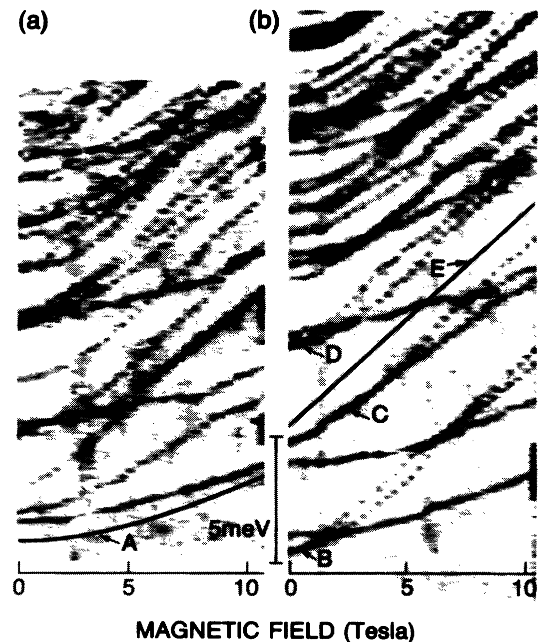

FIG. 4. (a),(b) Gray scale images of the sample capacitance as a function of energy and magnetic field. The vertical axis is derived from the gate bias. It corresponds to -600 mV at the bottom of the figure and to -500 mV at the top. Curve A is the theoretical result for the field dependence of a central D^0 state, and curve E represents the field dependence of the lowest Landau level, $\hbar\omega_c/2$.

distribution function multiplied by $-e/\eta C_{\text{shunt}}$ with the abscissa expanded by η. Consider the dc bias V_0 to be set at the center of a capacitance peak. Then, with added ac modulation, the quantum level in the well tends to be occupied during positive portions of the ac excitation and unoccupied during negative portions. Therefore, at zero temperature, the signal at the balance point is simply a square wave of variable duty cycle depending on the position of V_0 with respect to the center of the step.

At zero temperature, the signal after lock-in detection is a peak in the shape of half an ellipse [10] of height $\sqrt{2}e/\pi\eta C_{\text{shunt}}$ with a base width of twice the amplitude of the ac excitation, V_{ac}. At nonzero temperatures and for $V_{ac} < \eta k_B T/e$, the height of the peak drops and becomes amplitude dependent. For $V_{ac} \gg \eta k_B T/e$ the peak height saturates at $\sqrt{2}e/\pi\eta C_{\text{shunt}}$, and only its width increases.

Calculated line shapes for various values of V_{ac} are shown in the right inset of Fig. 3. These curves are convolutions of amplitude-dependent hemi-ellipses with the derivative of the Fermi distribution function scaled by η. In successive curves, V_{ac} is increased by a factor of 2. Our experimental data from a single isolated capacitance peak, shown in the central portion of Fig. 3, closely reproduce this dependence on V_{ac}. In order to achieve a satisfactory agreement between model calculation and experiment we had to adopt in Fig. 3 a sample temperature of $T=0.6$ K, somewhat warmer than the surrounding ^{3}He liquid at ≈ 0.35 K. It is likely that the 25 μW of power dissipated by the transistor which is thermally connected to the sample is responsible for this slight temperature rise in the tunnel capacitor.

The content of Figs. 2 and 3 establishes our ability to perform single-electron capacitance spectroscopy on discrete quantum levels. We find that the low-energy spectrum of our 1-μm disk consists of discrete electronic states with a characteristic energy spacing of a few meV. Such a large splitting cannot be caused by lateral confinement under the 1-μm disk. Instead, potential fluctuations in the quantum well must create local minima which localize the electrons into puddles. At high gate bias, the puddles merge and form the lowest two-dimensional band of the quantum well.

We now use our new spectroscopic tool to study the magnetic field evolution of the quantum states in the tunnel capacitor. Complete gate bias scans are taken at a sequence of fixed magnetic fields. After subtraction of a smooth background, we obtain a two-dimensional array of the sample capacitance as a function of magnetic field and gate bias. The capacitance is plotted in gray scale in which black represents the peaks. This representation allows us to follow the position of individual peaks with magnetic field. Figures 4(a) and 4(b) show such data from two separate runs between which the sample was thermally cycled.

All peaks of Figs. 4(a) and 4(b) start out with nearly

zero slope and move monotonically to higher gate bias with increasing magnetic field. The curves fall into two distinct classes characterized by their high-field slope. Most curves are of the steep-slope type. At high B fields the steep traces run nearly parallel to the line $E=\hbar\omega_c/2$, with ω_c being the cyclotron frequency. This is the magnetic field evolution of states which ultimately develop into the lowest Landau level. Their parabolic dependence at low fields reflects the lateral confinement of these levels. Most states cross over to a straight line at fields 0.5 $T<B<4.0$ T suggesting lateral confinement on the scale of the corresponding magnetic lengths l_0 of 360 Å $> l_0 >$ 130 Å. At these length scales the energy for the repulsion between two electrons in the same potential minimum is greater than $\sim$10 meV. Since the traces of Fig. 4 are much more closely spaced, they likely result from individual electrons tunneling into laterally separated unoccupied minima of the disorder potential.

We use a simple approximation to estimate the strength of the confining potential. The energy of the first electronic state in a cylindrically symmetric parabolic potential, of characteristic frequency ω_0, in a magnetic field is given by [11] $E=\hbar[(\omega_c/2)^2+\omega_0^2]^{1/2}$. We fit several of the curves in Fig. 4 by this expression and find in most cases that 0.3 meV $<\hbar\omega_0<$ 2.5 meV. The potential minima are probably created by fluctuations in the Si donor concentration.

The second class of curves, with a roughly parabolic dependence over the entire field range, follow closely the behavior of the lowest electronic state bound to residual hydrogenic impurities within the quantum well. These donors are probably Si dopant atoms which migrated up from the n^+ layer into the quantum well during MBE growth. Greene and Bajaj [12] have calculated the energy of these D^0 states in a GaAs quantum well. We observe several states whose field dependence agrees well with calculations for a D^0 state in which the impurity atom is near the well center [see Fig. 4(a)]. Others show a somewhat steeper field dependence consistent with states bound to impurities closer to the walls of the well.

There exists an intriguing feature of the data which is particularly apparent in Fig. 4(b). In several cases at zero magnetic field, two electrons enter the well at the same gate bias. This is apparent in curves B, C, and D which split into doublets at higher fields. This behavior may reflect accidental degeneracies. However, the fact that this phenomenon is observed for *all* those low-lying levels in Fig. 4(b) that are not bound to impurities, suggests a physical mechanism. Usually, electrons avoid entering the same potential minimum due to electron repulsion (Coulomb blockade). We observe the reverse. The transfer of one electron into the well causes a second to follow, although we cannot determine whether they occupy the same potential minimum. This behavior is reminiscent of an Anderson negative-U system [13], although we are unable to point to its origin.

In summary, we have demonstrated a spectroscopic tool for the study of discrete quantum energy levels. Application of this method to a small GaAs tunnel capacitor has yielded a measure of potential fluctuations in the device, the characterization of levels of individual impurity atoms, and the observation of unexpected degeneracies. Our single-electron capacitance spectroscopy will be applicable to a number of physics problems such as quantum dots, quantum rings, and defect levels.

We gratefully acknowledge helpful discussions with R. H. Silsbee, G. A. Baraff, H. F. Hess, H. D. Hallen, and T. J. Gramila.

[1] P. L. McEuen, E. B. Foxman, U. Meirav, M. A. Kastner, Yigal Meir, Ned S. Wingreen, and S. J. Wind, Phys. Rev. Lett. **66**, 1926 (1991).

[2] D. V. Averin and K. K. Likharev, in *Mesoscopic Phenomena in Solids*, edited by B. L. Altshuler, P. A. Lee, and R. A. Webb (Elsevier, Amsterdam, 1991).

[3] M. A. Reed, J. N. Randall, R. J. Aggarwal, R. J. Matyi, T. M. Moore, and A. E. Wetsel, Phys. Rev. Lett. **60**, 535 (1988).

[4] Bo Su, V. J. Goldman, and J. E. Cunningham, Science **255**, 313 (1992).

[5] Ch. Sikorski and U. Merkt, Phys. Rev. Lett. **62**, 2164 (1989).

[6] W. Hansen, T. P. Smith, III, K. Y. Lee, J. A. Brum, C. M. Knoedler, J. M. Hong, and D. P. Kern, Phys. Rev. Lett. **62**, 2168 (1989).

[7] R. C. Ashoori, R. H. Silsbee, L. N. Pfeiffer, and K. W. West, in *Nanostructures and Mesoscopic Systems*, edited by M. Reed and W. Kirk (Academic, New York, 1992), pp. 323–334.

[8] R. H. Silsbee and R. C. Ashoori, Phys. Rev. Lett. **64**, 1991 (1990).

[9] John Lambe and R. C. Jaklevic, Phys. Rev. Lett. **22**, 1371 (1969).

[10] R. C. Ashoori, Ph.D. thesis, Cornell University, 1991 (unpublished).

[11] C. G. Darwin, Proc. Cambridge Philos. Soc. **27**, 86 (1930).

[12] Ronald L. Greene and K. K. Bajaj, Phys. Rev. B **31**, 913 (1985).

[13] P. W. Anderson, Phys. Rev. Lett. **34**, 953 (1975).

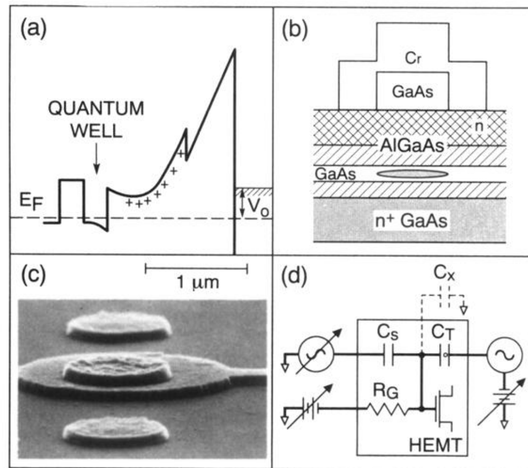

FIG. 1. (a) Conduction band profile of the multilayer sample. E_F is the Fermi level in the n^+ doped bottom layer. V_0 is the voltage applied to the gate. (b) Schematic cross section through the tunnel capacitor. (c) SEM photograph of the tunnel capacitor showing the top gate. (d) Low-temperature, on-chip capacitance bridge (box) and external circuit.

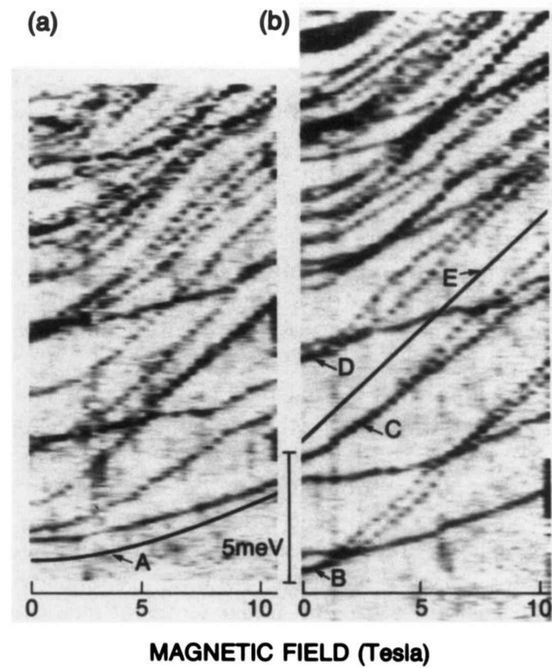

FIG. 4. (a),(b) Gray scale images of the sample capacitance as a function of energy and magnetic field. The vertical axis is derived from the gate bias. It corresponds to -600 mV at the bottom of the figure and to -500 mV at the top. Curve A is the theoretical result for the field dependence of a central D^0 state, and curve E represents the field dependence of the lowest Landau level, $\hbar\omega_c/2$.